

A Capacitor-Less CMOS Adaptively Biased Low-Dropout Regulator with Buffer for Portable On-Chip Application

WenTing Cui

School of Electronic and Information Engineering
Harbin Institute of Technology (ShenZhen)
ShenZhen, P.R. CHINA
cuixiaodou@yeah.net

PengFei Wang

R&D Department
CACHIP Tech
ShenZhen, P.R. CHINA
king0798@126.com

Yan Zhang

School of Electronic and Information Engineering
Harbin Institute of Technology (ShenZhen)
ShenZhen, P.R. CHINA
ianzh@foxmail.com

XianWei Zhang

School of Electronic and Information Engineering
Harbin Institute of Technology (ShenZhen)
ShenZhen, P.R. CHINA
13751060881@163.com

Abstract—This paper presents a capacitor-less low-dropout regulator (LDR), with adaptive bias (AB) and buffer structure for power management. Adaptive bias structure consists of current mirrors, which increase sensitivity for change of load current with low dissipation of small quiescent current, and make LDR more accurate. Buffer structure also consists of current mirrors and triode. By using the buffer, the stability of the LDR has been increased and the phase margin is over 54° with full range of load current from 100uA to 100mA. At maximum load current, the LDR's current efficiency is 99.50% with 1.8V power supply and 1.5V output. The power-supply rejection ratio at 1 kHz is 77.64dB with 1mA and -48.52dB with 100mA load current. The LDR Performance of the proposed LDR is verified with 0.11-um COMS process.

Keywords — *low-dropout regulator; adaptive bias; buffer; phase margin*

I. INTRODUCTION

Nowadays, with the development of intelligent lifestyle, people increasingly prefer to portable devices. Due to low dropout regulator (LDR) has simple structure, low cost, low power consumption and small size, it is widely used in portable electronic products^[1]. In portable products, the functions of products become versatile. At the same time, the power saving demand has been increased. Low power consumption not only means energy savings, also means extending the power cycle. In order to make the system work stability, traditional LDR adopts appropriate external capacitor to produce a zero for pole canceling in the LDR^[2]. This usually requires a large capacitor, also called equivalent series resistance^[3], which is not only wasting of resources but also increasing costs, while weakening the portability features of portable devices^[4]. The output voltage level will change by following the load current

^[5], the error amplifier (EA) is used to sense the change of current and the power transistor will be driven to compensate this change. However, there is a delay between the EA reaction and the output current change, causing voltage spikes and reducing the accuracy of the circuit^[6]. There are many factors that cause the delay and parasitic capacitors of the LDR is one of the main reasons^[7]. It is difficult to have a good trade-off among the LDR loop bandwidth, stability and quiescent current.

Because of these challenges, in this paper, a low-voltage capacitor-less adaptively biased LDR with buffer is presented. This structure extends the loop bandwidth and improves the stability of the circuit. Since the power consumption change follows the load current^[8], the circuit consumes very little quiescent current under no load conditions. Because high-precision LDR requires high loop gain^[9], this design uses two-stage amplifier under low power supply voltage.

The organization of this paper is given as follows: Section II presents the structure of the LDR and discusses its overall performance. Section III simplifies the circuit and obtain a model to analyze the main feedback loop (MFL). Section IV presents the simulation results respectively, Section V concludes the design efforts.

II. THE PROPOSED LDR STRUCTURE AND IT'S PERFORMANCE ANALYSIS

The generalized architecture of the proposed LDR with the structure of AB and buffer is shown in Fig.1. Schematic diagram consists of the following basic parts: the current bias circuit, bandgap reference voltage source, an error amplifier, AB structure, buffer structure, the output regulator and the feedback resistor. Current bias circuit provides high accuracy and low temperature drift current^[10]. Bandgap reference provides the reference voltage V_{REF} for the LDR. Error amplifier compares the feedback voltage

of the output of LDR with the V_{REF} , and amplifies the difference to control the regulator, so to maintain a stable output voltage V_{out} . The source voltage V_{DD} of LDR is 1.8V. The positive input of the differential amplifier V_{REF} is 1V, and the output of LDR is 1.5V. Adaptive bias structure is introduced in the differential amplifier. Adaptive bias structure is implemented by a simple current mirror. Bias circuit provides a large bias current for EA when loads is heavy to maintain a large loop bandwidth^[11]. And at light load it provides a small bias current to maintain high current efficiency. Miller capacitor C_M is used to split the pole which are located at the output of EA and the output of LDR^[12]. And Q-reduction capacitor C_Q is used to reduce I_{load} ^[13]. In this paper two-stage EA is used to achieve high bandwidth and high gain. Operational trans-conductance amplifier (OTA) has high gain and low bandwidth characteristic and is used as the main EA^[14]. The second OTA amplifier which based on a smaller gain and larger bandwidth is mainly used to monitor the output of the LDR. The third gain stage of the LDR is power transistor M_P . Since the pass transistor has a large parasitic capacitor, the EA which has a small quiescent current produces a low frequency pole at output stage of the LDR. Application of buffer isolates the high output impedance of the output stage of EA and the high load capacitor of M_P , pushing zero of right half plane and improving PSRR of the LDR^[15]. Two-stage EA is composed of $M_0 \sim M_8$. Bias current is composed of M_{ab1} , M_{ab2} , $M_{a1} \sim M_{ab3}$. Buffer is composed of M_{ab1} , M_{ab2} , $M_{b1} \sim M_{b1}$, M_{B3} . M_{B4} and Q_0 . Miller capacitor C_M connects the output of the first stage EA and the output terminal the LDR, Q-reduction capacitor connects gate and drain of M_6 , while also connects M_3 and M_4 . Under no load condition, Power transistor works in the cut-off region and the quiescent current consumption of the LDR is small. At light load condition, the rest circuit work in sub-threshold region, except the differential amplifier circuit. In this case, leakage current of M_1 is approximately $6 \mu A$, and current is supplied by M_{a3} and is almost zero, only $156 nA$. As the load current increases to approximately $25 \mu A$, M_P works into saturation region from sub-threshold region. At this point, the rest of the circuit in addition to the M_{a3} located in the linear region which provides dynamic bias current for differential amplifier, and the rest of the LDR circuits are in saturation region. M_{a3} in the linear region can be more sensitive to provide compensation current to the differential amplifier with the load current dynamic changes.

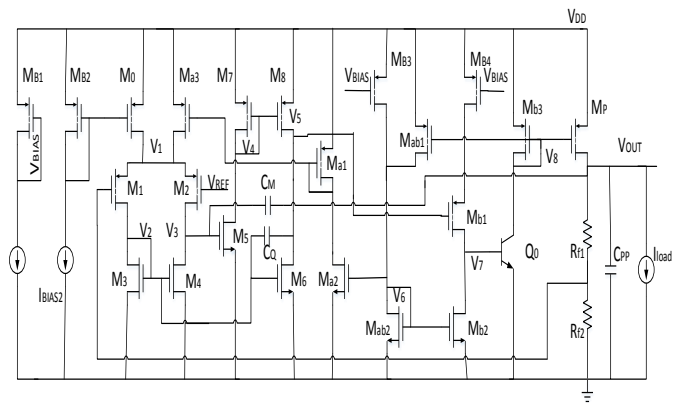


Fig.1. Schematic of the LDR with AB and buffer structure

M_{ab2} and M_0 provide a fixed bias current for EA. M_{B1} provides bias voltage for M_{B3} and M_{B4} . The implementation of adaptive bias circuit provides dynamic current for the differential circuit consists of three current mirror: (M_{a3} , M_{a1}), (M_{ab2} , M_{a2}), (M_P , M_{ab1}). The ratios of current mirror are $M_{a3} : M_{a1}$ (1:1), $M_{ab2} : M_{a2}$ (40:1), $M_P : M_{ab1}$ (248:1). Fixed current combination adaptive bias current form are used in buffer structure. Among them, M_{B3} and M_{B4} provide fixed bias current for buffer. The current mirror consists of M_P and M_{b3} have the same ratio as $M_P : M_{ab1} \cdot M_{b1}$ as a source follower, when it is lightly loaded in sub-threshold region. There are three main circuit poles. The first pole P_1 is located at the EA's output N_1 , The second pole P_2 is located at the buffer's output N_2 . And P_1 is less sensitive to the LDR's load current than the pole P_2 . The output pole P_3 is located at the LDR's output V_{out} . The pole P_1 is mainly determined by the output impedance of EA and the equivalent capacitor of N_1 . The pole P_2 is mainly determined by the output impedance of buffer and the input capacitor of M_P . The pole P_3 is mainly determined by the equivalent impedance and load capacitor of the output of LDR. The pole P_3 is more sensitive to the change of the load current than the pole P_2 . Larger load current would push P_3 to higher frequency more than push P_2 to high frequency. The equivalent capacitor of N_1 point and the output impedance of the buffer should be small, making the pole P_1 and P_2 located at very high frequency and circuit become a single pole frequency response. The output impedance of buffer is

$$R_{ob} = 1 / [g_{mb1}(1 + \beta) + g_{mb3}] \quad (1)$$

g_{mb1} is the transconductance of transistor M_{b1} . g_{mb3} is the transconductance of transistor M_{b3} , β is the current gain of triode Q_0 . The value of β of this design

is 10. When the load current increases, g_{mb1} and g_{mb3} all will increase, leading to the value decrease. The load current increase also makes P_2 throughout the load current range located in a very high frequency, which is greater than unity gain frequency. Since the M_{ab1} 's V_{DS} is larger than M_p 's V_{DS} , the sense current of M_{b3} will change larger than the load current.

The adaptive bias structure and buffer structure also improve the slew-rate of this circuit. When the load current increase, M_{ab1} and M_{b3} follow M_p to increase currents, thus the current of M_{a3} and M_{b1} increase. The increase of current of M_{a3} and M_{b1} will increase the collector current of Q_0 . Gate voltage of M_p will decrease when the collector current of Q_0 increase. At the same time, it increases a parasitic capacitor's discharge current and the slew-rate of circuit. The enhancement of slew-rate can speed up the transient response of the LDR^[16].

III. STABILITY ANALYSIS OF CIRCUIT

The main feedback loop (MFL) transfer function of the LDR is presented for stability analysis, Fig. 2 is a small-signal model of the circuit main loop.

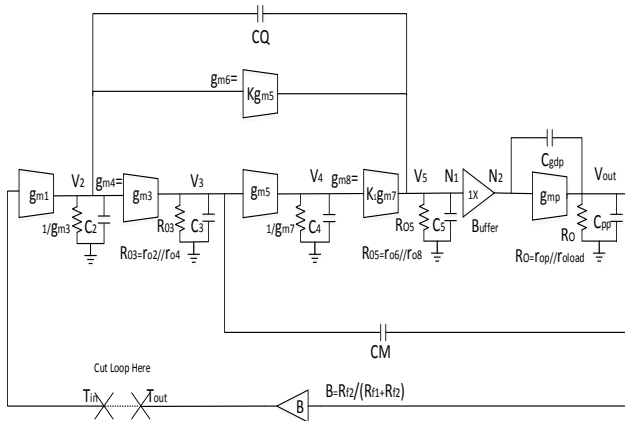


Fig. 2. Small signal model of the LDR MFL

B represents the circuit feedback factor. g_{m1} , g_{m3} , g_{m5} , g_{m6} , g_{m7} , g_{m8} , g_{mp} represent the transconductance of each transistor. Based on the following considerations, the loop gain transfer function is presented as follows:

1) The parasitic capacitor from $V_2 \sim V_5$ is $C_2 \sim C_5$, in the stability analysis, the value of $C_2 \sim C_5$ is very small, and the corresponding frequency is much greater than the UGF. Therefore, the parasitic capacitor $C_2 \sim C_5$ in the calculation can be ignored. And because the power transistor M_p is very large, the value of C_{gdp} can't be ignored.

2) Power transistor M_p provides the third stage gain is $Gain_3 = g_{mp} R_o$. $Gain_3$ follows the load current I_{load} change. Their specific relationship is $Gain_3 \propto \sqrt{I_{load}}$.

3) Buffer structure with an impedance value is represented by R_{ob} where in (1).

Based on the above considerations, the LDR loop gain transfer function is:

$$T(s) = \frac{T_{out}}{T_{in}} \approx A_{MFL} \times \frac{1+a_1s+a_2s^2+a_3s^3+a_4s^4+a_5s^5}{1+b_1s+b_2s^2+b_3s^3+b_4s^4+b_5s^5+b_6s^6} \quad (2)$$

With:

$$A_{MFL} = -B g_{m1} R_{o3} g_{m6} R_{o5} g_{mp} R_o \quad (3)$$

$$a_1 = \frac{C_M (g_{m6} R_{o5} g_{mp} - g_{m3})}{g_{m3} g_{m6} R_{o5} g_{mp}} + \frac{C_{gdp} g_{m3}}{g_{mp} R_{o5} R_{ob}} + \frac{C_M g_{m3} R_{o3}}{R_o R_{o5} R_{ob}} \quad (4)$$

$$a_2 = \frac{C_M^2 R_{o3} + C_M C_{gdp} R_{ob}}{g_{mp} g_{m6} R_{o5}} + \frac{C_Q C_M + C_{gdp} C_M R_{o3}}{g_{m6} g_{mp}} + \frac{C_M C_Q (1+R_{o3})}{g_{m3} g_{m6}} + \frac{C_M^2}{g_{m1} g_{m6}} \quad (5)$$

$$a_3 = \frac{C_{gdp} C_M C_Q R_{o3}^2}{g_{m3} g_{mp}} + \frac{C_M C_Q^2}{g_{m3}^2 g_{m6}^2 g_{m1}} + \frac{R_{o3} g_{m3} C_M + C_{gdp} g_{m3}}{g_{m3} g_{mp} g_{m1} g_{m6}^2} + \frac{C_M^2 C_Q}{g_{m6}^2 g_{m1} g_{mp}} \quad (6)$$

$$a_4 = \frac{C_{gdp} C_M^2 C_Q R_{o3}}{g_{mp} g_{m3}^2} + \frac{C_M^2 C_Q^2 R_{o3}}{g_{m3}^2 g_{m6}} + \frac{C_{gdp} C_M^2 C_Q R_{o3}}{g_{mp} g_{m3} g_{m6}} + \frac{C_{gdp} C_M^2 C_Q R_{o3} R_{ob}}{g_{mp} g_{m6}} \quad (7)$$

$$a_5 = \frac{C_{gdp} C_M^2 C_Q^2 R_{o3}}{g_{mp} g_{m6} g_{m3}} \quad (8)$$

$$b_1 = C_M g_{m6} g_{mp} R_{ob} R_{o5} R_{o3} \quad (9)$$

$$b_2 = C_M C_Q (R_{o3} + R_{o5}^2) + C_M C_{gdp} (R_o R_{ob} + R_{o3} R_o + 1) + C_M C_{PP} + C_{PP} C_{gdp} R_o R_{ob} \quad (10)$$

$$b_3 = \frac{C_M C_Q C_{gdp} (R_o R_{ob} + R_{o5} R_{o3})}{g_{m3}} \quad (11)$$

$$b_4 = \frac{R_{o3} R_o C_Q C_{gdp} C_M + R_{o3}^2 C_M^2 C_{gdp} C_Q}{g_{m3}} \quad (12)$$

$$b_5 = \frac{R_{o3}R_{ob}R_oC_Q^2C_{gdp}C_M C_{PP}}{g_{m3}} + \frac{R_{o5}^2R_oC_M^2C_{gdp}C_Q C_{PP}}{g_{m3}} + \frac{R_{o3}^2R_oC_{PP}^2C_{gdp}C_Q C_M}{g_{m6}} \quad (13)$$

$$b_6 = (C_M^2C_Q^2C_{gdp}C_{PP}R_{o3}^2R_{ob}R_oR_{o5})/g_{m3} \quad (14)$$

From (2), (3) and (9), The unity gain bandwidth can be obtained as follows $w_{UGF} = Bg_{m1}/C_M$, the denominator is 6 order polynomials, showing that there are six poles. Poles which varies with load impedance R_o can be clearly seen (10) ~ (14). Under the light load conditions, though g_{mp} is small, the value of R_o is large. Because of $g_{mp}R_o \propto 1/\sqrt{I_{load}}$, under the light load conditions, the DC gain is larger and PSRR is larger as well. Large PSRR means smaller ripple.

When the load current $I_{load} = 0$, g_{mp} is small, and the leakage current of transistor M_p is least. Buffer is used to reduce the output impedance. The value of C_5 can be decreased by reducing the size of M_{b1} at $I_{load} = 0$ which UGF is located at higher frequency and better phase margin is obtained. When I_{load} increases, g_{mp} also increases and the second pole also increases. The phase margin and stability become better.

Under no load condition, the quiescent current of this LDR consumption of 163.4uA. At this time, UGF is 1.57MHz and phase margin is 54°. With the increase of load current, UGF and the phase margin also increases. When the load current at maximum is 100mA, the quiescent current is 500uA, and the UGF is 1.66MHz. Compared to no buffer structure at the LDR circuit, UGF increase to 0.46MHz.

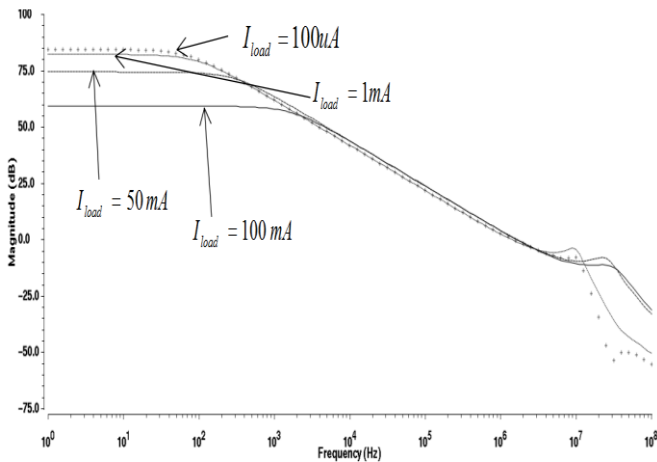


Fig. 3. The MFL simulation amplitude waveform

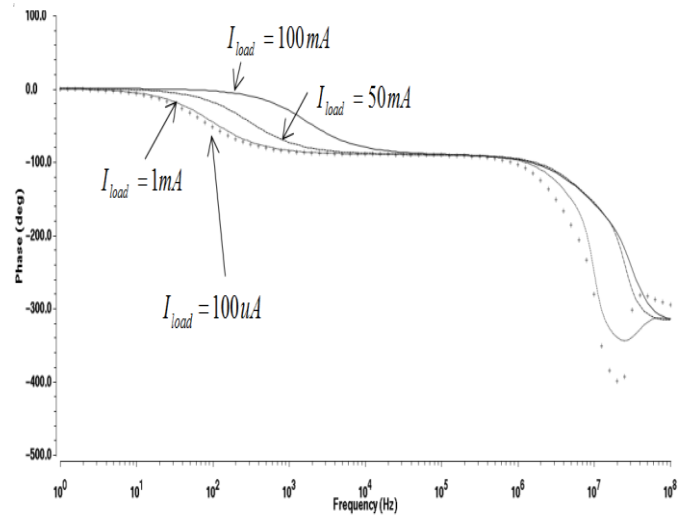
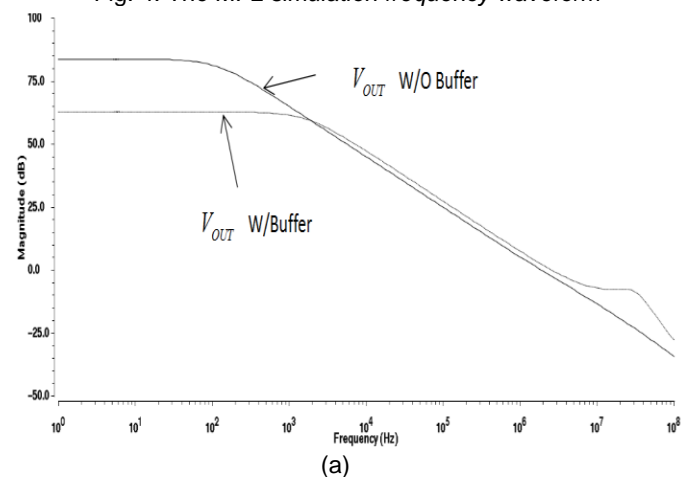
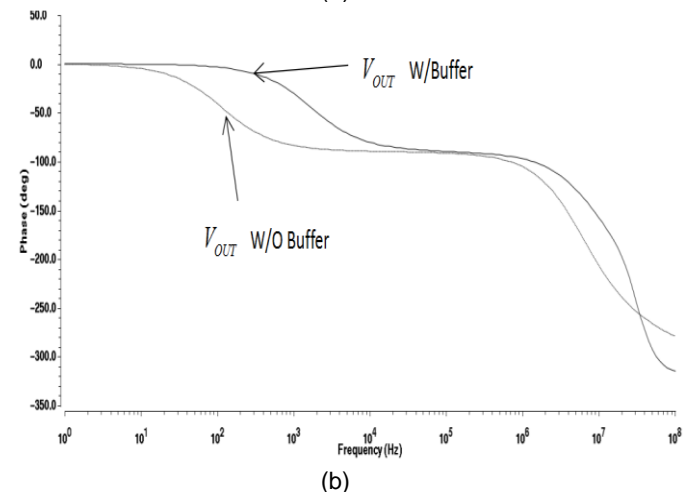


Fig. 4. The MFL simulation frequency waveform



(a)



(b)

Fig. 5. The frequency responses waveform at 100mA load with and without buffer: (a) amplitude waveform (b) frequency waveform

The simulations is shown in Fig. 3 and 4 to illustrate the loop gain of the frequency response curve. It can be seen from figure 6, the first and second pole are pushed to the outside of the unit gain bandwidth. When the load current changes from 100uA to 100mA, all phase margin is larger than 45°. When the load current is 100uA, the phase margin is 54°, gain is 85.24dB; when the load current is 100mA, the phase margin is 77° and gain is 59.03dB.

It can meet the gain requirements of the LDR's EA and achieve good stability performance.

In Fig.5, it's shown that after adding buffer structure, the gain becomes smaller. The reason is that the buffer structure reduces the output impedance. It is generally understood that amplifier gain can be written as the $A_v = g_m R_o$. Compared to the no buffer circuit, the gain with buffer circuit become smaller for the R_o become smaller. In Fig.6, it is shown that the LDR with buffer structure phase margin is higher than that without buffer structure. For the reason that R_o becomes smaller, the corresponding pole is pushed to outside of unit gain bandwidth which is located at the frequency that higher than without buffer structure. So this structure is more stable.

IV. SIMULATION RESULTS

The proposed LDR with buffer and AB structure is designed by using a standard 0.11- um CMOS process. The value of the compensation capacitor and Q-reduction capacitor are both 10 pF. The parasitic capacitor of the LDR is assumed to be 100 pF in the simulations. Table I shows the performance of the proposed LDR with buffer and AB structure.

TABLE I. THE SUMMARY OF THE LDR PERFORMANCE

Technology	HHGRACE 0.11-um 2P4M CMOS
V_{DD}	1.8V-5V
V_{REF}	1V
V_{out}	1.5V
I_{load}	100uA-100mA
C_{PP}	100pF
$C_M \cdot C_Q$	10pF, 10pF
Line Reg. @100mA	1.0mV/V
Load Reg. @1.8V	6.01uV/mA
Line Tran. ΔV_{out} (2.3-2.0V@100mA)	-11mV/+1mV 2.5us
Load Tran. ΔV_{out} (1-50mA@1.8V)	-553mV/+191mV 0.7us
PSR@1kHz, 1mA	-77.64dB
PSR@1kHz, 50mA	-65.61dB
PSR@100kHz, 1mA	-22.02dB
PSR@100kHz, 50mA	-24.26dB

As shown in Table I, the range of power supply V_{DD} is between 1.8 and 5V, the EA's positive input V_{REF} is 1V, and the LDR's output V_{out} is 1.5V. The maximum load current is 100mA. For dynamic performance, the line regulator is 1.0mV/V at 100mA load current and the load regulator is 6.01uV/mA at 1.8V power supply. When I_{load} is 100mA V_{DD} is be

changed from 2.3V to 2.0V in 2.5us and the transient error voltage of V_{out} is within 11mV. The load transient response is measured with load current from 1mA to 50mA at V_{DD} =1.8V, and the undershoot (overshoot) voltage is 553 mV (191mV). At 1Hz frequency, the light load current have better PSRR than heavy load. But the PSRR with 50 mA is better than that with 1 mA under 100kHz. The reason is that the influence of parasitic capacitor and load capacitor become remarkable in high frequency.

V. CONCLUSIONS

In this paper, the LDR with buffer and AB structure is proposed. The AB structure is sensitive to the change of load current and increase the accuracy of the LDR. The buffer structure attenuates the output resistance which drives the power transistor and pushes the pole at the gate of the power transistor to higher frequency. The AB structure and buffer structure also improve the slew-rate and speed up the transient response of the LDR. Experiment results show that the proposed LDR has good stability and PSRR. The AB structure improves the transient response of the LDR. Simultaneously, it can ensure the enough phase margin and maintain the stability of the LDR under heavy load conditions. Buffer structure further improves the stability of the LDR under the full range of load currents. And internal compensation capacitor can be as small as 10pF without external capacitor. Capacitor-less LDR with adaptively biased and buffer structure can reduce the chip area of portable devices and have more stable performance.

REFERENCES

- [1] Hamed Aminzadeh, Mohammad R. Nabavi and Wouter A. Serdijn. Low-dropout voltage source: An alternative approach for low-dropout voltage regulators [J]. IEEE Transactions on Circuits and Systems II: Express Briefs, Vol.61 (6) 2014, pp.413-417.
- [2] Robert J. Milliken, Jose Silva-Martínez and Edgar Sánchez-Sinencio. Full on-chip CMOS low-dropout voltage regulator [J]. IEEE Transactions on Circuits and Systems-I: Regular Papers, Vol. 54, NO. 9, SEPTEMBER 2007, pp.1879-1889.
- [3] Marco Ho, Jianping Guo, Kai Ho Mak, A CMOS low-dropout regulator with dominant-Pole substitution[J]. IEEE Transactions on Power Electronics, Vol. 31, NO. 9, September 2016, pp.6362-6369.
- [4] Yat-Hei Lam, Wing-Hung Ki, Chi-Ying Tsui. Adaptively-biased capacitor-less CMOS Low dropout regulator with direct current feedback[C]. Asia and South Pacific Conference on Design Automation, 2006, pp.104-105.
- [5] Saad Bin Nasir, Samantak Gangopadhyay, and Arijit Raychowdhury. All-digital low-dropout regulator with adaptive control and reduced dynamic stability for digital load circuits [J].

IEEE Transactions on Power Electronics, Dec. 2016, Vol.31 (12), pp.8293-8302.

[6] Chenchang Zhan and Wing-Hung Ki. An output-capacitor-free adaptively biased low-dropout regulator with subthreshold undershoot-reduction for SoC[J]. IEEE Transactions on Circuits and Systems I: Regular Papers, May 2012, Vol.59 (5), pp.1119-1131.

[7] Chenchang Zhan and Wing-Hung Ki. Output-capacitor-free adaptively biased low-dropout regulator for system-on-chips [J].IEEE Transactions on Circuits and Systems I-regular Papers, v. 57, (5, Sp. Iss. SI), 2010, MAY, pp.1017-1028.

[8] Chenchang Zhan and Wing-Hung Ki. Output-capacitor-free adaptively biased low-dropout regulators[C]. 2010 IEEE International Conference of Electron Devices and Solid-State Circuits (EDSSC), Dec. 2010, pp.1-4.

[9] Ashis Maity and Amit Patra. Design and analysis of an adaptively biased low-dropout regulator using enhanced current mirror buffer [J]. IEEE Transactions on Power Electronics, March 2016, Vol.31 (3), pp.2324-2336.

[10] Jae-Mun Oh, Byung-Do Yang, Hyeong-Ju Kang, et al. 250 mV supply voltage digital low-dropout regulator using fast current tracking scheme[J]. ETRI Journal, Vol 37, Number 5, October 2015, pp.961-969.

[11] Ashis Maity and Amit Patra. Trade-offs aware design procedure for an adaptively biased capacitorless low dropout regulator using nested miller compensation [J]. IEEE Transactions on Power Electronics, VOL. 31, NO. 1, January 2016, pp.369-380.

[12] [12] Zhang Gengyu, Xiao Xia, Nie Kaiming ,et al. Low-power three-stage amplifier using active—feedback miller capacitor and serial RC frequency compensation[C]. Tianjin University and Springer-Verlag Berlin Heidelberg 2015, 21.pp.515-523.

[13] Sai Kit Lau, Philip K. T. Mok and Ka Nang Leung. A low-dropout regulator for SoC with Q-reduction [J]. IEEE Journal of Solid-State Circuits, Vol. 42, NO. 3, March 2007, pp.658-663.

[14] Chung-Hsun Huang, Ying-Ting Ma, and Wei-Chen Liao. Design of a low-voltage low-dropout regulator[J] IEEE Transactions on Very Large Scale Integration, June 2014, Vol.22(6), pp.1308-1313.

[15] Mohammad Al-Shyoukh, Hoi Lee and Raul Perez. A transient-enhanced low-quiescent current low-dropout regulator with buffer impedance attenuation [J]. IEEE Journal of Solid-State Circuits, Vol. 42, NO. 8, August 2007, pp.1732-1741.

[16] Edward N. Y. Ho and Philip K. T. Mok. A capacitor-less CMOS active feedback low-dropout regulator with slew-rate enhancement for portable on-chip application [J]. IEEE Transactions on Circuits and Systems—II: Express Briefs, Vol. 57, NO. 2, 2010, pp.80-84.